Production Engineering
https://doi.org/10.1007/s11740-023-01186-7

QUALITY

In-situ characterization of tool temperatures using in-tool integrated thermoresistive thin-film sensors

Germán González[1] · Marcel Plogmeyer[2,3] · Julius Schoop[4] · Günter Bräuer[2] · Volker Schulze[1]

Received: 30 September 2022 / Accepted: 20 January 2023

Abstract
Metal cutting is characterized by high temperatures at the tool-workpiece interface. Although valuable information could be provided by the temperature values, their direct measurement still presents a challenge due to the high contact pressure and the inaccessibility of the process kinematic. In this research work, the current state of thin-film sensors for measuring temperatures on the chip-tool interface has been analyzed with a focus on the measuring phenomena: thermoelectricity and thermoresistivity. Thin-film sensors placed on the cutting tools in or close to the tool-chip contact area are expected to obtain accurate temperature information at the expense of a short lifetime. New insights into thin-film sensors manufacturing, design and calibration are presented, and a new concept of a three-point thermoresistive thin-film sensor is proposed. During orthogonal cutting tests the workpiece deformations were measured through high-speed imaging and the process temperatures were measured with thin-film sensors. In order to validate the temperatures and to obtain the temperature distribution on the cutting edge, Finite Element simulations were carried out. Finally, the potential of using cutting tools with integrated thin-film sensors for in-situ characterization is investigated and a statement for its limitations and potential applications is given.

Keywords Thin-film sensor · Orthogonal cutting · High-speed imaging · Temperature measurement

1 Introduction

The objective of this manuscript is to present a method for combining thin-film sensor technology with high-speed imaging in an in-situ characterization orthogonal cutting setup to measure process-specific induced strain and mechanical loads of the machined workpiece and temperature gradients in the cutting tool. With the aid of high fidelity in-situ characterization techniques that are capable of measuring thermo-mechanical loads imposed during cutting processes, machining can be meaningfully integrated within the paradigm, which seeks to unify materials and manufacturing science across the complex production chain [1]. When attempting to study machining processes, careful consideration of the fundamental process physics is required to select suitable characterization and modeling approaches. At the most basic level, there are three major deformation zones in machining, namely primary, secondary and tertiary deformation zones (PDZ, SDZ, and TDZ). The thermo-mechanical loads imposed on the cutting tool and workpiece material are often extreme, with large strains ($\epsilon > 1$), high strain rates ($\dot{\epsilon}$) of more than $10^5\ s^{-1}$ in certain cases (e.g., finish machining with rounded edge tools), as well as high temperatures ($T = 200 - 1000°C$) and extreme temperature gradients of up to 100 K/s [2, 3]. While shearing the workpiece to remove a controlled amount of material, machining processes typically induce severe plastic deformation (SPD) on the chip and the machined (sub-)surface, which may significantly alter the machined workpiece's microstructure and material properties [4]. Moreover, the thermal and mechanical loads are often coupled, and the resulting thermo-mechanical processing can affect the surface integrity of the workpiece material to depths ranging from 10 to

✉ Germán González
german.gonzalez@kit.edu

1 wbk Institute of Production Science, Karlsruhe Institute of Technology (KIT), Kaiserstr. 12, Karlsruhe 76131, Germany

2 Institute for Surface Technology (IOT), TU Braunschweig, Bienroder Weg 54E, Braunschweig 38108, Germany

3 Fraunhofer Institute for Surface Engineering and Thin Films IST, Bienroder Weg 54E, Braunschweig 38108, Germany

4 Department of Mechanical Engineering, University of Kentucky, 143 Graham Ave, Lexington, Kentucky 40506, USA

Published online: 31 January 2023

1000 microns, depending on the material properties, tool geometry, cooling/lubricating condition, and process parameters [5, 6]. Understanding of the underlying fundamental process physics allows the Surface Conditioning oriented [7] machining processes, i.e. the transition from the geometry-focused paradigm towards a paradigm of using machining to control location-specific properties and have the potential to enable location-specific control over process-induced material properties (e.g., microstructure and residual stresses) and performance (e.g., fatigue life) in machined components. This demands a better understanding of machining processes in the context of the chip formation mechanisms, surface integrity, induced strain, and temperature measurement of the machined workpiece, chip, and cutting tool.

In the present manuscript, the state of the art of thin-film sensor technology applied to temperature measurement on cutting tools is presented, as well as a new design of temperature thin-film sensor based on resistance thermometers for their use in combination with high-speed imaging for in-situ characterization of the chip formation process. The working principle, manufacturing process, calibration, and validation procedures are explained. Tool temperature gradients measured by the thin-film sensors were cross-validated with Finite Element (FE) chip formation simulations using the measured workpiece deformations and mechanical loads as calibration variables. The results provide an insight into the potential of using thin-film sensors for in-situ characterization during plane strain linear sliding and its application in the development of inverse modeling approaches.

1.1 Heat generation in metal cutting

Most workpiece material properties are temperature-dependent functions. A given machined workpiece can react quite differently at low temperatures (typically low cutting speeds) and high temperatures (typically higher cutting speeds and feeds) [8]. To understand these temperature-dependent effects, it is crucial to develop in-situ temperature monitoring techniques to better analyze the generation, distribution, and heat effects (and their resulting temperature) in metal cutting operations. Figure 1 shows a two-dimensional orthogonal cutting representation with the primary sources of heat generation in the cutting process that have been identified as being associated with three key locations: the primary shear zone, the tool-chip interface (secondary deformation zone), and the flank-workpiece interface (tertiary deformation zone).

The tool-chip interface, the secondary shear zone, generates heat due to the frictional effect of the sliding chip on the cutting tool. Heat is generated at the flank-workpiece interface due to the frictional contact between the tool and the workpiece. In contrast, heat is dissipated at the primary shear zone due to plastic deformation [9]. Existing

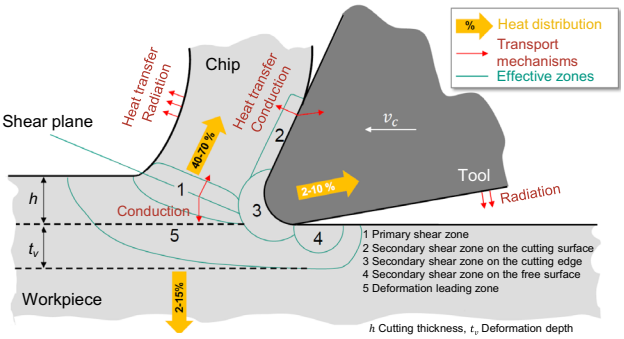

Fig. 1 Two dimensional representation of the heat transfer mechanism and heat partitioning during the cutting process

temperature measurement techniques are performed either in-situ or post-process (for instance observation of metallurgical changes and thermal painting). Measuring cutting temperatures directly and reliably is notoriously complicated to implement. These techniques can be grouped into conduction and radiation techniques. Conduction techniques measure temperature based on the temperature difference between two surfaces that are in direct contact. In contrast, radiation technology measures the electromagnetic radiation on each body surface relative to its temperature. The conduction techniques (consisting of thermocouple, temperature lacquer, and coated structures) can be divided into either thermoelectric or thermochemical effects depending on their operating principle [10].

2 Temperature measurement using thin-film sensors

The measurement of localized temperatures during the cutting process can be carried out without affecting process performance using suitable thin-film sensors integrated into the cutting tools with high temporal and spatial resolution as shown by Basti et al. during the orthogonal machining of A6061-T6 aluminum alloy [11]. Thin films are produced by a process technology known as micro-electromechanical systems (MEMS). The material is directly deposited with a thickness in the micron- to nanometer range onto the cutting tool surface, usually in a vacuum deposition chamber by physical vapor deposition (PVD) (e.g. sputtering, thermal evaporation) or by chemical deposition (e.g. plating, chemical vapor deposition (CVD)) [12]. The sensor layers are patterned using lithography, etching, laser structuring or shadow masks. The combination of multiple stacked layers forms the thin-film system. Each one of these layers provides different properties such as isolation, wear resistance as well as sensory properties like thermoelectricity

or thermoresistivity , which are the main thermal measuring principles used by thin-film technology [13]. Both are graphically represented in Fig. 2. The sensor lies between two layers of insulation on a carbide substrate. A final layer protects the insulation layers against wear and oxidation. The measurement principles of both sensor types as well as their characteristics are explained in the following sections and summarized in Table 1.

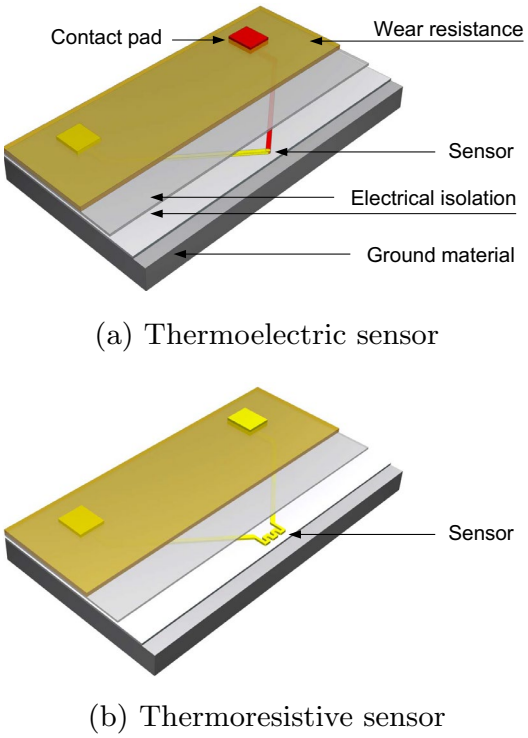

Fig. 2 Classification of thin-film sensor technologies according to the measuring principle

2.1 Thermoelectric thin-film sensors

The thermoelectric effect, also called Seebeck effect, describes the generation of a voltage due to a temperature difference between the electrical junctions of two different conductors. The voltage is dependent on the difference in the material's Seebeck coefficients and is approximately proportional to the temperature difference. Sensors based on this effect are called thermocouples. Weinert et al. [14] used micro-milled masks and an arc PVD process for coating the rake face of ceramic silicon nitride turning inserts with three conductive pairs of Ni and NiCr paths, and they were tested during the dry turning of cast alloy GG25. However, the application of thin metallic PVD layers on silicon nitrides features an insufficient adhesion due to the lack of diffusive bonding during coating and the different thermal expansion coefficients of materials during cooling after the coating process. The sensors were not protected against chips or flowing material, so the cutting depth was selected according to that, measuring temperatures up to 150 °C. Biermann et al. [15] continued working with the same sensor design, including a wear-protection layer of Al_2O_3 above the sensor paths. The authors investigated the effect of the mask thickness, the path width, and the path geometry, proving that they directly affect the sensor performance. The sensors were tested

Table 1 Overview of thermoelectric (TE) and thermoresistive (TR) thin-film sensors in machining

Measuring principle	Substrate	Adhesion promoter	Isolation	Sensor material	Isolation & wear protection	Test material	References
TE	Si_3N_4	–	–	Ni / NiCr	–	GG25	[14]
TE	Si_3N_4	–	-	Ni / NiCr	Al_2O_3	GJL-600	[15]
TE	Si_3N_4	–	-	Ni / NiCr	–	β-titanium	[16]
TE	PCBN	Ti	Al_2O_3	WRe 5/26	–	AISI O_2	[17]
TE	WC-Co	Cr	Al_2O_3	Ni / NiCr	Al_2O_3 + TiN	AISI 12L14	[18]
TE	Al_2O_3	–	–	Ni / NiCr	HfO_2 + TiN	A6061	[11]
TE	Al_2O_3 + ZrO_2	–	–	Pt13%Rh-Pt	Al_2O_3 + AlN	AISI 1045	[19]
TE	Al_2O_3	–	–	Cu / CuNi	Si_3N_4	A5056	[20]
TE	WC-Co	–	Al_2O_3	WC-Co / Cr	–	MC Nylon	[21]
TE	HSS	–	SiO_2	NiSi / NiCr	SiO_2	Aluminum	[22]
TE	AISI H11	TiAlN	Al_2O_3	Ni / NiCr	Al_2O_3	–	[23]
TE	WC-Co	–	–	NiCr/NiAl	Si_3N_4	β-titanium	[24]
TE	PCBN	Ti	Al_2O_3	WRe 5/26	–	Ti_6Al_4V	[25]
TR	Diamond	–	–	Pt	–	AlMg	[26]
TR	Diamond	–	–	Pt	Glass	AlMg	[27]
TR	WC-Co	Ti	Al_2O_3	Cr	Al_2O_3	AISI 4140	[28]

during the turning process of gray cast iron material GJL-250 and GJL-600, measuring temperatures up to 200 °C. The sensors were calibrated using two methods: By heating the workpiece during the turning process with a torch and measuring the temperature in the tool with thermocouples, as well as by submerging the tool tip in an oil bath with controlled temperature. Tillmann et al. [16, 29] using the same manufacturing strategy, studied the effect of the monolayer thickness and coatings composition on the wear properties of the PVD layer. It was concluded that the Cr-CrN material combination presents higher wear resistance and micro hardness. The main problems of the thin-film thermocouples were also investigated: Delamination, flake, and geometrical inaccuracies as the effect of the ground material surface roughness on the adhesion of the coating. Werschmoeller et al. [17] investigated the capability of high-temperature materials such as tungsten-5% rhenium and tungsten-26% rhenium for the manufacturing of thermocouples and tested them in orthogonal cutting experiments of AISI-O_2. The sensors were integrated into the cutting tool by diffusion bound and placed on the flank face, parallel to the cutting process plane. The sensors measured temperatures up to 900 °C and showed a response time of fewer than 150 ns. Kesriklioglu et al. [18] developed a thin-film sensor composed of a thin layer of chromium sputtered on the rake face of a WC-Co insert as an adhesion promoter to form a compatible interface between the ground material and one Al_2O_3 dielectric layer. K-Type thin-film thermocouple conductive paths were located 30 µm to the cutting edge. Another coating followed the thermocouple fabrication process with Al_2O_3 to prevent a shortcut between the measurement junction and the AlTiN protective layer. The sensors were tested during the oblique interrupted cutting test with 12L14 steel. Basti et al. [11] also manufactured a thin-film sensor system made of Ni-(Ni-Cr) thermocouples protected by an Al_2O_3+AlN or TiN layer and insulated with a layer of HfO_2 using PVD and photolithography on the rake face of alumina tools, under the chip-tool contact surface at 0.3 mm distance from the cutting edge. The sensors were tested during orthogonal cutting of A6061-T6 aluminum alloy. The response time was 300 ms and measured maximum temperatures of 620 °C. Shinozuka et al. [19, 20] also deposited thin-film sensors made of seven pairs of built-in micro Cu-CuNi thermocouples on the rake face of carbide tools 600 µm away from the cutting edge. Still, they made micro-grooves on the rake face of alumina tools with ultrasonic machining to embed the conducting paths through electroless plating. The Cu-Ni thermocouples were then protected against wear with a Si_3N_4 coating. The sensors were tested during the longitudinal turning of A5056 aluminum alloy. Since the micro thermocouples were set in the grooves, the sensors' endurance was higher than those placed on a plane and polished rake face. Sugita et al. [21] continued with the idea of an array of micro thermocouples integrated on the tool's rake face and placed into grooves. The groves were manufactured utilizing laser milling and coated with an insulating film of Al_2O_3 and with conductive paths of Cr. On the measuring point, there is no insulating coating. Thus the Cr comes into contact with the cutting tool ground material, made of cemented carbide, leading to a (WC-Co)-chromium (Cr) thermocouple. The WC-Co itself forms the cutting tool, and the sensor has a characteristic feature that it can be miniaturized. WC-Co is one of the main components of a cutting tool, and it produces a high negative thermoelectric power. The sensors were tested during the turning of MC Nylon. Cui et al. [22] placed SiO_2 insulating film, NiCr/NiSi thermocouple film and SiO_2 protecting film on the surface of HSS substrates. Bobzin et al. [23] developed a thin-film sensor system composed of a TiAlN+Al_2O_3 insulation layer deposited on the cutting tool made of 1.2343 hot work tool steel, a Ni-NiCr thermocouple and an Al_2O_3 wear protective and insulating layer. A novel characterization method was presented using a heat plate and measuring the temperature with an external thermocouple and an infrared camera. Li et al. [24] manufactured six pairs of Ni-Cr/Ni-Al conductive paths on grooves on the rake face of tungsten carbide-cobalt cutting inserts in the chip-tool contact area and protected them with a film of Si_3N_4. In following investigations of the same working group C-type sensors consisting of tungsten-26%rehenium (W/Re26) and tungsten-5%rehenium (W/Re5) were tested on PCBN tools for machining of Ti_6Al_4V and their durability was investigated, resulting in an increase in tool life compared to thin film sensors placed on a flat surface without grooves [25].

2.2 Thermoresistive thin-film sensors

Resistance thermometers use the temperature dependence of the electrical resistance. There are two types: Positive temperature coefficient materials (PTCs), where resistance increases with increasing temperature due to thermal oscillations of ions impeding their movement, and negative temperature coefficient materials (NTCs), where resistance decreases with increasing temperature due to an increase in free electrons from the valence band as a result of thermal excitation. Most pure metals belong to the first type. Yoshioka et al. [26] mounted a platinum resistance microsensor directly on the rake face of a single crystal diamond tool tip for in-process temperature monitoring during ultraprecision turning of Al-Mg alloy. It was able to detect the thermal behavior with a quick response and a high resolution because of the small heat capacity and short heat transfer delay of the sensor. Hayashi et al. [27] continued this work with a new design of the resistive sensor, evolving from a zig-zag design to a meander shape, and improving the measuring strategy using a resistance bridge, an amplifier, and a low pass filter to detect the

changes in the output voltage. In the authors' previous research, Cr was used as a sensor layer. It was placed between two isolation Al_2O_3 layers on the rake face of cemented carbide cutting inserts. Their functionality was tested in turning experiments of AISI 4140, showing a fast response time and a maximum measured temperature of 250 °C [28].

3 Design and manufacturing oriented to high-speed imaging applications

High-speed imaging and digital image correlation techniques have been established as a reliable method for measuring the strain and strain rates of the workpiece during the machining process [30]. Since the focus of this research work relays on the thin-film technology, the fundamental concepts of the high-speed imaging will not be addressed. This section explains the considerations that have to be taken for design and manufacturing a thermoresistive thin-film sensor placed on a tool, which will be used in posterior high-speed imaging experiments. The main objective is therefore the acquisition of the combined data of temperature gradients on the chip-tool interface, cutting forces, chip formation and surface microstructure evolution.

3.1 Sensor design

Micro-sized chromium-based thermoresistive thin-film sensors were mounted on the rake face of squared uncoated carbide inserts for use in orthogonal cutting experiments. The sensor design is based on previous own works [28] and it was adapted to the requirements of the high-speed imaging experiments. The right side of the tool and the workpiece need to be on the same plane. Therefore, the nose radius of the cutting tool was trimmed using electrical discharge machining (EDM) and subsequently polished for obtaining a parallel face to the workpiece. Afterward, the tools were cleaned in an ultrasonic bath of acetone and isopropyl alcohol. In-situ observation of the cut is carried out on this plane under the assumption of plane strain deformation conditions. Three gauge elements are located close to the cutting edge allowing the measurement of the temperature of the chip-tool contact area with high resolution and fast response. The gauge elements are aligned horizontally to the cutting edge such that they will be centered in front of the workpiece. They have a distance of 100 µm from each other and are placed as close as 100 µm to the cutting edge. Their width is about 30 µm. Sensors are numbered 1 to 3 starting with the one closest to the cutting edge.

3.2 Thin-film system fabrication

3.2.1 Deposition

At first, an insulation layer of Al_2O_3 with a thickness of 3.5 µm was deposited onto the inserts through PVD. It was followed by sputtering of a 100 nm thin chromium layer. After structuring, a second Al_2O_3 layer of 2 µm thickness was deposited on top of it for insulation and wear-protection purposes. When the calibration process finished, a mask was applied and the contact pads were coated with a copper layer so that wires could be soldered to them.

3.2.2 Structuring

The result of the structuring process was improved as compared to previous work concerning the minimal distance of the gauge elements to the cutting edge. Photolithography and wet-chemical etching were still used, but instead of spray coating or spin coating the photoresist, which often leads to an inhomogeneous coating on edges, was applied by electrophoretic deposition (EPD). The main advantages of EPD are the possibility of coating complex geometries such as the sharp cutting edge of a cutting tool and a very uniform coating thickness without porosity. In the EPD process, the resist particles form micelles, which have a charged surface in an electrolyte. By applying a voltage between the substrate and a surrounding electrode, the resist micelles migrate to the substrate and deposit on its surface. The resist has an isolating effect so that this reaction stops by itself when the entire substrate is covered, thus enabling the advantages mentioned above. By this modified structuring process, gauge elements can be positioned as close as 100 µm to the cutting edge.

3.3 Calibration process

In previous own investigations, the calibration of the thin-film sensors is limited to a maximum temperature of 170 °C when using wires previously soldered to the sensor due to the melting point of the soldering material. Therefore, a new test rig was implemented in this work which allows calibration up to 400 °C. The coated inserts were placed on a hot plate and surrounded by metallic masking to limit the cooling caused by the surrounding temperature (see Fig. 3a). Two sets of wires link the sensor element to the monitoring device as shown in Fig. 3b. Instead of soldered wires, spring probes were mounted on the contact pads of the insert. To measure all three sensors of a single insert at the same time, a PTFE construction was designed to fix twelve spring probes at the right distances to each other. On their other end, the spring probes were wired to the measuring devices. The surface reference temperature was recorded by using a commercial PT100 sensor which was placed on the position

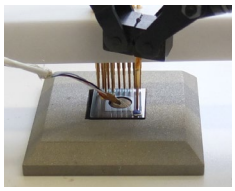

(a) Sensor calibration

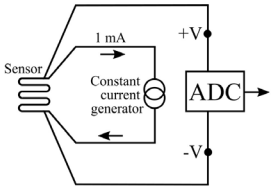

(b) 4-wire configuration.

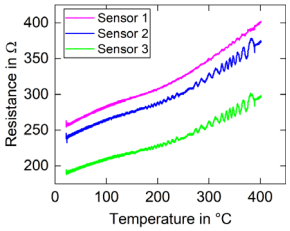

(c) Thermoresistive characteristic for three sensors on the same tool.

Fig. 3 Calibration procedure and contacting

of the three sensors. Figure 3c shows the thermoresistive characteristic. It can be described by the following function:

$$R(T) = R_0 \cdot [1 + \alpha \cdot (T - T_0) + \beta \cdot (T - T_0)^2] \quad (1)$$

The temperature coefficients α and β as well as the output resistance R_0 at temperature $T_0 = 0\,°\text{C}$ were determined for each sensor. On average, the values of the temperature coefficients are $\alpha = 1.0 \cdot 10^{-3}\,1/\text{K}$ and $\beta = 1.2 \cdot 10^{-6}\,1/\text{K}^2$.

3.4 Contacting and electronics

A four-wire configuration, as shown in Fig. 3b, was used for measuring the voltage in the sensor generated by the sensor resistance increment produced by temperature changes. One set delivers the constant current used for measurement (e.g. 1 mA), and the other set measures the voltage drop over the resistor. This wiring configuration is the most accurate for measuring a Resistance Temperature Detector (RTD). Shielded wires were soldered to the sensors and covered with epoxy for protection against the chips after the calibration. With this configuration the resistance of the measuring element is not affected by the resistance of the leads and wires. A Raspberry Pi® Model 4B was combined with a voltage measurement MCC118 DAQ HAT from Measurement Computing with a 12-bit resolution and 100 kS/s sampling rate. A constant current source HAT has been developed able to convert the 5.1 V from the Raspberry Pi® into three constant current outputs of 1.00 mA. Temperatures are calculated from the measured voltages using the thermoresistive

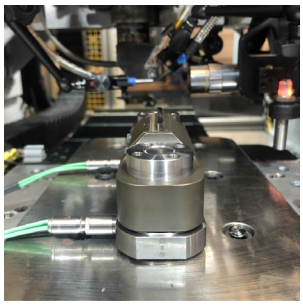

(a) In-situ testbed

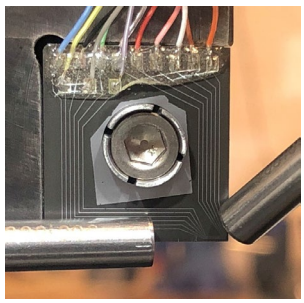

(b) Thin-film sensor

Fig. 4 Testbed for in-situ characterization at the University of Kentucky

characteristic and additionally filtered with a digital 25 Hz low-pass filter to improve the signal-to-noise ratio.

4 Experimental setup

Dry orthogonal linear cutting tests were conducted on a custom-built testbed for ultra high-speed in-situ experimental characterization under plane strain condition. The setup shown in Figure 4 features a cutting tool with rake angle γ of -5 degrees, clearance angle α of 5° and a sharp cutting edge r_β of 5 µm, coated with a thin-film sensor system and mounted on a Coromant Capto C3®, on the vertical axis, which controls the uncut chip thickness h. A linear motor is used for the horizontal axis movement where the workpiece holder and two piezoelectric force sensors are clamped as shown in Fig. 4a. The horizontal system features positional repeatability of better than 0.4 µm. Cuboid shape AISI 4140 specimens with a hardness of 36 HRC were precision machined to a length of 60 mm and a thickness of 3 mm by means of EDM and ground and polished in order to obtain a residual stresses free volume and a very flat surface respectively. The tests were carried out combining cutting speeds $v_c = 30 - 120$ m/min and uncut chip thicknesses $h = 50 - 100$µm. Cutting forces are measured using two uniaxial ring force transducers placed under the workpiece holder. Temperatures are measured on three points of the tool rake face using thin-film sensors. The chip formation phenomenon is captured using a high-speed camera, focused to the plane where the workpiece, tool and most part of the chip are found, as shown in Fig. 5a. The camera sensor, optics, lighting and operative settings such as frames per second, magnification and exposure time used in the experiments are described in detail in [30]. The obtained images had a resolution of 640x640 pixels with a pixel size of 2 µm. The shear angle ϕ, the uncut chip thickness h, and

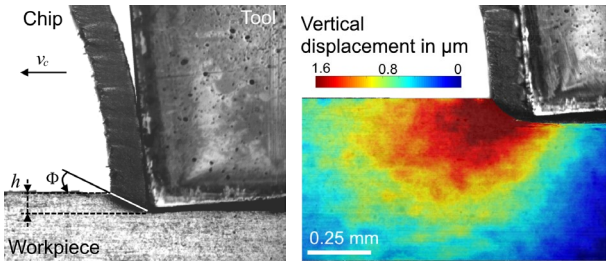

(a) In-situ high-speed image. (b) Image post-processed with ncorr DIC software.

Fig. 5 In-situ high-speed imaging and post-processing: 10x objective magnification, 159 ns exposure, $v_c = 120$ m/min, $h = 100$ µm

the chip geometry can be obtained directly from the high-speed image. By means of Digital Image Correlation (DIC) the workpiece deformations and strains were obtained as shown in Fig. 5b. For this analysis the software MATLAB® with the 2D digital image correlation program ncorr [31] were used.

5 FE Simulations

Finite Element (FE) simulations were conducted with the software Simufact Forming 21.0. with the aim of temperature cross-validation with the thin-film sensors. For the modelling of the workpiece material, the von Mises plasticity and the Johnson-Cook (JC) flow stress equation were used. Orthogonal cutting was simulated as a two dimensional process with a plain strain assumption and an explicit time integration. The simulation featured a rigid tool and rigid coating fixed in the space with heat transmission, and an elasto-plastic workpiece. Furthermore an Arbitrary Lagrange Eulerian formulation with a frequent workpiece remeshing was used, which resulted in a minimum element edge length of 1 µm. A thermal conductivity of 3 W/m·K were obtained experimentally with the 3ω method according to [32] for the Al_2O_3 coating material. A constant coating thickness value of 5 µm was tactile measured and a specific heat capacity of 0.9 J/g°C was obtained from literature [32]. The chip-tool surface temperature will differ from the measured temperature due to the Al_2O_3 coating. The temperature along the coating was obtained from the FE simulations. By simulating the most severe process parameters of this study, maximum temperature deviations between tool surface and sensor of 30 °C were obtained.The JC constants were calibrated according to [33] using the measured cutting forces and the max. workpiece displacements obtained from the DIC software as objective values. The resulting JC parameters

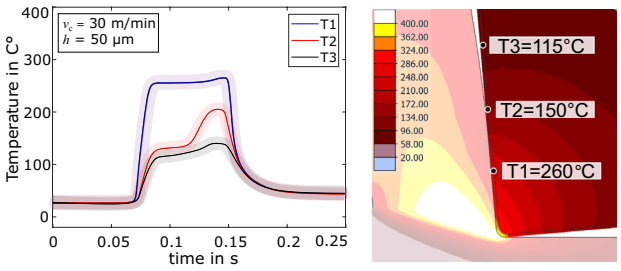

(a) Thin-film sensors measurement. (b) FE simulated temperatures.

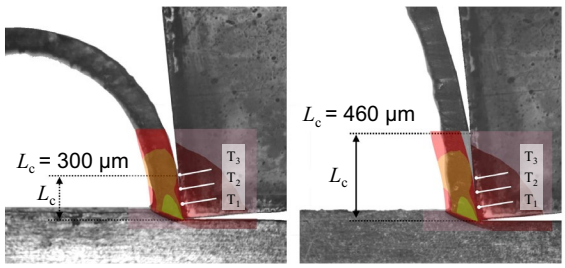

(c) Chip formation process at the start and at the end of the cut. Overlap with FE simulated temperatures for appreciation of the error in the contact length, Lc. $v_c = 60$ m/min, $h = 100$ µm.

Fig. 6 Thin-film measurements analyse and cross-validation with FE simulations

used in this work were: $A = 620$ MPa; $B = 660$ MPa; $C = 0.023$; $m = 0.975$; $n = 0.119$. The friction of the system was described using a temperature independent combined Coulomb-Shear friction model. The Coulomb factor value µ and the shear factor value m were calibrated at 0.35 and 0.70 respectively. The temperatures along the tool rake face after a simulated cutting path of 5 mm were compared with the experimental measured temperatures and for predicting a value of the maximum tool temperature.

6 Results and discussion

The function and service life of the thin-film sensors, as well as the capability of the test bench to measure temperature, forces and the chip formation were studied under the different parameter combinations. In Fig. 6 an overview of the temperature measurements and its comparison with the FE simulations is given. Figure 6a shows the temperatures obtained from the thin-film sensor signal in time domain. The signal of the first sensor, located a 100 µm from the cutting edge, shows steady-state behaviour and rapid response time. The signal of the second sensor however presents a remarkable increment in temperature at the end of the cut.

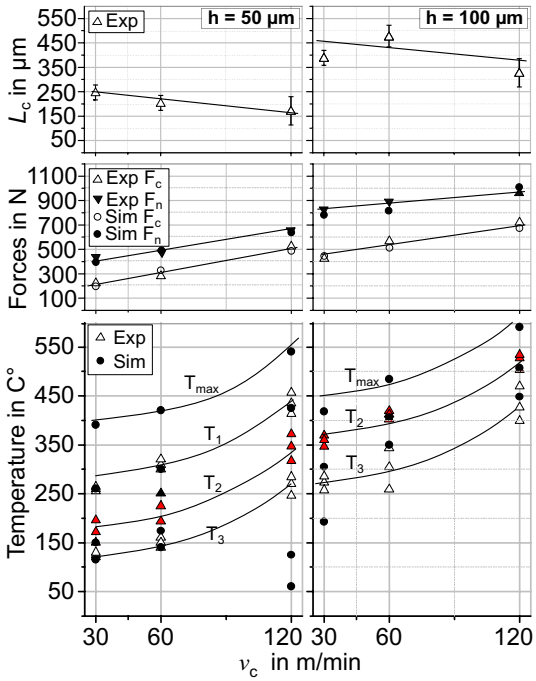

Fig. 7 Experimentally and simulative obtained forces, contact lengths and rake face temperatures during orthogonal cutting of AISI 4140

This phenomenon was observed in a high percentage of the measurements. FE simulations were used for cross-validation of the temperature gradient on the tool rake face and to predict the maximum temperature on the tool. High-speed imaging was used for explaining the lack of steady state observed. Figure 6b shows the temperature results of the FE simulation with the process parameters $v_c = 30$ m/min, $h = 50$ µm. Here it is observed that the measured temperatures do not correspond with the maximum tool temperature. It is also observed that the values measured by the first sensor have a value very similar to the values obtained by the simulation. The values obtained by the second sensor, due to the lack of steady-state, are difficult to compare with the simulation results. An explanation for the non-stationary character of the measurements is proposed with the aid of Fig. 6c. Here two high-speed images are shown, which belong to the 1/4 and 3/4 of the workpiece machined length. The same simulated temperature gradient overlaps both images. Here it can be appreciated how the chip formation phenomena cannot be correctly modeled during the entire cutting process, with variations of the chip-workpiece contact length up to 200%. This leads to a variation on the predicted temperature gradients that is going to affect mainly even the measured temperatures by the second and third thin-film sensor.

Figure 7 shows the results of the experimental tests and the simulations. Here the measured temperatures by the thin-film sensors are compared with FE simulations. The maximum temperature on the tool obtained from the simulations is also provided. For the selected process parameters the maximum tool temperatures are found on the tool tip, as shown in Fig. 6b. Thereby the temperatures curves T_{max}, Temperature on the tool tip; T_1, at 100 µm from the cutting edge; T_2, at 200 µm from the cutting edge; and T_3, at 300 µm from the cutting edge; were obtained. Experimental temperature values present more repeatability when the sensor is closer to the secondary shear zone on the cutting edge, which varies strongly with the uncut chip thickness. This can be appreciated in the high repeatability of the curves T_1, h = 50; and T_2, h = 100 µm. The simulated temperatures loose accuracy with increasing the distance to the cutting edge. Strong deviation in the simulated temperatures are related directly with inaccuracies in the simulation of the chip formation, in particular the chip-tool contact length, L_c. It has to be mentioned that this deviation has not a significant influence on the simulated cutting forces as shown in Fig. 7.

7 Conclusions

A novel thermoresistive thin-film sensor system was developed and integrated into a tool insert for its application into an in-situ characterization testbed, allowing to measure temperatures at three positions on the rake face of the tool in the chip-tool contact area, as well as the cutting forces, the chip formation, and the workpiece deformations using force sensors, high-speed imaging and digital image correlation respectively. The sensors were tested during orthogonal cutting of AISI 4140 alloy steel and cross-validated with FE simulations. Some key findings include:

- The presented thin-film sensors are able to measure the temperatures on the rake face of cutting tools closer to the cutting edge than any other sensor that can be found in the current literature.
- The obtained measurements can help to model the cutting process more accurately. The 4-wire configurations of the presented RTD sensors offer more accurate measurements than the sensors based on Seebeck effect (thermocouples).
- The control period of life of the sensors, added to the complexity of their manufacturing, makes their integration in the industrial field difficult, but the quality of the information that they allow to obtain makes them a high-quality measurement.
- Through the variation of sensor design temperatures can be obtained in the desired areas of the tool or even the workpiece.

- The sensor design also allows the detection of tool wear, which can make this sensor another ally for condition monitoring during machining.

The development of more accurate ways to obtain information from the machining process is expected to significantly improve the understanding of the relaying mechanism of the chip formation as well as the tool wear. Future and ongoing work will focus on the studying and modelling of the microstructural development of different workpiece materials during machining with the aid of the valuable and spatially resolved information provided by the thin-film sensors.

Acknowledgements The authors gratefully acknowledge the financial support of the the Karlsruhe House of Young Scientists (KHYS) and the German Research Foundation, Deutsche Forschungsgemeinschaft (DFG) within the research priority program SPP2086 "Surface Conditioning in machining" SCHU 1010/63-2 and BR 2178/47-2, with the project number 401538720.

Funding Open Access funding enabled and organized by Projekt DEAL.

Declarations

Conflict of interest The Authors declare that they have no conflict of interest.

References

1. Doghri I, Lemoine G, Martiny P, Mathieu S, Wucher B, Adam L (2021) Multiscaling-based integrated computational materials engineering: from academia to industry. Int J Multiscale Comput Eng 19(4):1–40
2. Denkena B, de Leon L, Koehler J (2010) Influence of scaled undeformed sections of cut on strain rate, cutting force and temperature. Prod Eng 4:457–464. https://doi.org/10.1007/s11740-010-0230-9
3. Childs THC (2010) Surface energy, cutting edge radius and material flow stress size effects in continuous chip formation of metals. CIRP J Manufact Sci Technol 3(1):27–39. https://doi.org/10.1016/j.cirpj.2010.07.008
4. Jawahir IS, Brinksmeier E, M'Saoubi R, Aspinwall DK, Outeiro JC, Meyer D, Umbrello D, Jayal AD (2011) Surface integrity in material removal processes: recent advances. CIRP Ann 60(2):603–626. https://doi.org/10.1016/j.cirp.2011.05.002
5. la Monaca A, Murray JW, Liao Z, Speidel A, Robles-Linares JA, Axinte DA, Hardy MC, Clare AT (2021) Surface integrity in metal machining - part ii: functional performance. Int J Mach Tools Manufact 164:103718. https://doi.org/10.1016/j.ijmachtools.2021.103718
6. Liao Z, la Monaca A, Murray J, Speidel A, Ushmaev D, Clare A, Axinte D, M'Saoubi R (2021) Surface integrity in metal machining - part i: fundamentals of surface characteristics and formation mechanisms. Int J Mach Tools Manufact 162:103687. https://doi.org/10.1016/j.ijmachtools.2020.103687
7. Stampfer B, González G, Gerstenmeyer M, Schulze V (2021) The present state of surface conditioning in cutting and grinding. J Manufact Mater Process. https://doi.org/10.3390/jmmp5030092
8. Komanduri R, Hou ZB (2000) Thermal modeling of the metal cutting process: Part i - temperature rise distribution due to shear plane heat source. Int J Mech Sci 42(9):1715–1752. https://doi.org/10.1016/S0020-7403(99)00070-3
9. Rech J, Arrazola PJ, Claudin C, Courbon C, Pusavec F, Kopac J (2013) Characterisation of friction and heat partition coefficients at the tool-work material interface in cutting. CIRP Ann 62(1):79–82. https://doi.org/10.1016/j.cirp.2013.03.099
10. Davies MA, Ueda T, M'Saoubi R, Mullany B, Cooke AL (2007) On the measurement of temperature in material removal processes. CIRP Ann 56(2):581–604. https://doi.org/10.1016/j.cirp.2007.10.009
11. Basti A, Obikawa T, Shinozuka J (2007) Tools with built-in thin film thermocouple sensors for monitoring cutting temperature. Int J Mach Tools Manufact 47(5):793–798. https://doi.org/10.1016/j.ijmachtools.2006.09.007
12. Espinosa HD, Zhu Y, Moldovan N (2006) Mems-based material testing systems. In: Buschow KHJ, Cahn RW, Flemings MC, Ilschner B, Kramer EJ, Mahajan S, Veyssière P (eds) Encyclopedia of Materials: Science and Technology, pp 1–10. Elsevier, Oxford. https://doi.org/10.1016/B0-08-043152-6/02136-7. https://www.sciencedirect.com/science/article/pii/B0080431526021367
13. Dinh T, Phan H-P, Qamar A, Woodfield P, Nguyen N-T, Dao DV (2017) Thermoresistive effect for advanced thermal sensors: Fundamentals, design considerations, and applications. J Microelectromech Syst 26(5):966–986. https://doi.org/10.1109/JMEMS.2017.2710354
14. Weinert K, Tillmann W, Hammer N, Kempmann C, Vogli E (2006) Tool coatings as thermocouple for the monitoring of temperatures in turning processes. Adv Eng Mater 8(10):1007–1010. https://doi.org/10.1002/adem.200600122
15. Biermann D, Kirschner M, Pantke K, Tillmann W, Herper J (2013) New coating systems for temperature monitoring in turning processes. Surf Coat Technol 215(10):376–380. https://doi.org/10.1016/j.surfcoat.2012.08.086
16. Tillmann W, Vogli E, Nebel J (2007) Deposition of multi-functional coatings by physical vapour deposition. Mater Sci Forum 539–543:1194–1199. https://doi.org/10.4028/www.scientific.net/MSF.539-543.1194
17. Werschmoeller D, Li X, Ehmann K (2012) Measurement of transient tool-internal temperature fields during hard turning by insert-embedded thin film sensors. J Manufact Sci Eng. https://doi.org/10.1115/1.4007621.061004
18. Kesriklioglu S, Arthur C, Morrow JD, Pfefferkorn FE (2019) Characterization of tool-chip interface temperature measurement with thermocouple fabricated directly on the rake face. J Manufact Sci Eng. https://doi.org/10.1115/1.4044035.091008
19. Shinozuka J, Obikawa T (2004) Development of cutting tools with built-in thin film thermocouples. Key Eng Mater 257–258:547–552. https://doi.org/10.4028/www.scientific.net/KEM.257-258.547
20. Shinozuka J, Binti Jaharadak H (2016) Measurement of the temperature distribution at the tool-chip interface by using a cutting

tool with seven pairs of built-in micro cu/ni thermocouples. Adv Mater Res 1136:586–591. https://doi.org/10.4028/www.scientific.net/AMR.1136.586
21. Sugita N, Ishii K, Furusho T, Harada K, Mitsuishi M (2015) Cutting temperature measurement by a micro-sensor array integrated on the rake face of a cutting tool. CIRP Ann 64(1):77–80. https://doi.org/10.1016/j.cirp.2015.04.079
22. Cui YX, Sun BY, Ding WY, Sun FD (2009) Development of multilayer composition thin film thermocouple cutting temperature sensor based on magnetron sputtering. Adv Mater Res 69–70:515–519. https://doi.org/10.4028/www.scientific.net/AMR.69-70.515
23. Bobzin K, Brögelmann T, Kruppe NC, Janowitz J (2020) Temperature measurement on tool surfaces by wear resistant pvd sensor coatings. Defect Diffus Forum 404:138–145. https://doi.org/10.4028/www.scientific.net/DDF.404.138
24. Li J, Tao B, Huang S, Yin Z (2018) Built-in thin film thermocouples in surface textures of cemented carbide tools for cutting temperature measurement. Sens Actu A Phys 279(2):663–670. https://doi.org/10.1016/j.sna.2018.07.017
25. Li T, Shi T, Tang Z, Liao G, Han J, Duan J (2020) Temperature monitoring of the tool-chip interface for pcbn tools using built-in thin-film thermocouples in turning of titanium alloy. J Mater Process Technol 275(2):116376. https://doi.org/10.1016/j.jmatprotec.2019.116376
26. Yoshioka H, Hashizume H, Shinno H (2004) In-process microsensor for ultraprecision machining. Sci Measure Technol IEE Proc 151:121–125. https://doi.org/10.1049/ip-smt:20040375
27. Hayashi M, Yoshioka H, Shinno H (2008) An adaptive control of ultraprecision machining with an in-process micro-sensor. J Adv Mech Design Syst Manuf 2:322–331. https://doi.org/10.1299/jamdsm.2.322
28. Plogmeyer M, González G, Schulze V, Bräuer G (2020) Development of thin-film based sensors for temperature and tool wear monitoring during machining. tm - Technisches Messen 87(12):768–776. https://doi.org/10.1515/teme-2020-0058
29. Tillmann W, Vogli E, Herper J, Biermann D, Pantke K (2010) Development of temperature sensor thin films to monitor turning processes. J Mater Proc Technol 210(5):819–823. https://doi.org/10.1016/j.jmatprotec.2010.01.013
30. Schoop J (2021) In-situ calibrated modeling of residual stresses induced in machining under various cooling and lubricating environments. Lubricants. https://doi.org/10.3390/lubricants9030028
31. Blaber J, Adair B, Antoniou A (2015) Ncorr: open-source 2d digital image correlation matlab software. Experim Mech 55(6):1105–1122
32. Lee S-M, Cahill DG, Allen TH (1995) Thermal conductivity of sputtered oxide films. Phys Rev B 52:253–257. https://doi.org/10.1103/PhysRevB.52.253
33. Stampfer B, González G, Segebade E, Gerstenmeyer M, Schulze V (2021) Material parameter optimization for orthogonal cutting simulations of aisi4140 at various tempering conditions. Proc CIRP 102, 198–203. https://doi.org/10.1016/j.procir.2021.09.034. (18th CIRP Conference on Modeling of Machining Operations (CMMO), Ljubljana, Slovenia, June 15-17, 2021)